

Effects of wavelength-dependent fluence attenuation on the noninvasive photoacoustic imaging of hemoglobin oxygen saturation in subcutaneous vasculature *in vivo*

Konstantin Maslov¹, Hao F Zhang^{1,2} and Lihong V Wang

¹ Optical Imaging Laboratory, Department of Biomedical Engineering, Washington University in St. Louis, Campus Box 1097, One Brookings Drive, St. Louis, MI 63130, USA

² Department of Electrical Engineering and Computer Science, University of Wisconsin - Milwaukee, PO Box 748 Milwaukee, WI 53201-0784, USA

E-mail: lhwang@biomed.wustl.edu

Received 2 April 2007, in final form 16 October 2007

Published 23 November 2007

Online at stacks.iop.org/IP/23/S113

Abstract

Quantitative measurements of the oxygen saturation of hemoglobin (sO_2) in a blood vessel *in vivo* presents a challenge in photoacoustic imaging. As a result of wavelength-dependent optical attenuation in the skin, the local fluence at a subcutaneous vessel varies with the optical wavelength in spectral measurement and hence needs to be compensated for so that the intrinsic absorption coefficient can be recovered. Here, by employing a simplified double-layer skin model, we demonstrate that although the absolute value of sO_2 in a vessel is seriously affected by the volume fraction of blood and the spatially averaged sO_2 in the dermis, the difference of sO_2 between neighboring vessels is minimally affected. Experimentally, we acquire compensational factors for the wavelength-dependent optical attenuation by measuring the PA spectrum of a subcutaneously inserted 25 μm thick black film using our PA microscope. We demonstrate *in vivo* that the difference in sO_2 between a typical artery and a typical vein is conserved before and after spectral compensation. This conservation holds regardless of the animal's systemic physiological state.

Introduction

Photoacoustic (PA) imaging is based on the detection of the laser-induced ultrasonic waves, which are resulted from optical absorption and thermoelastic expansion. The PA images, acquired by either reconstruction-based photoacoustic tomography (PAT) [1–5] or direct photoacoustic microscopy (PAM) [6–8], describes the internal distribution of the optical

¹ These authors contributed equally to this work.

energy deposition (specific absorption), which is the product of the local fluence and the local optical absorption coefficient. As a result, PA images are well suited to reveal optical absorption contrast but, at the same time, can be biased in depicting tissue's optical absorption coefficient distribution if there is a large variation in local fluence. The local fluence varies with the optical wavelength, in addition to optical heterogeneity, owing to the wavelength-dependent optical absorption and reduced optical scattering coefficients in the surrounding tissue, such as the skin. Therefore, compensating for the spectral variation in the local fluence is required to recover the intrinsic optical absorption coefficient.

A spectral measurement of the intrinsic optical absorption coefficient can provide quantitative imaging of functional parameters, such as the oxygen saturation of hemoglobin (sO_2). In PA imaging of sO_2 in subcutaneous vessels, spectral measurement is employed to extract the relative concentrations of both the oxyhemoglobin (HbO_2) and deoxyhemoglobin (HbR) on the basis of their distinctive optical extinction coefficient spectra.

To measure sO_2 correctly, we must compensate for the effect of spectral variations in the local fluence. We can choose a spectral range—for example, between 650 nm and 850 nm, where optical attenuation in the skin is relatively low—to minimize the spectral variations in the local fluence. However, within this spectral range, the signal-to-noise ratio is relatively low because of the low optical absorption of blood in targeted vessels.

A straightforward compensation method is to employ a skin model and an independent optical measurement so that the optical properties in the skin can be measured and, thus, the spatial and spectral variations of the local fluence can be estimated. However, this approach, which has not yet been reported, requires simultaneous implementation of two different experimental techniques.

Several methods have been developed to measure sO_2 in both *in vitro* and *in vivo* samples using PA measurements only [9–11]. In [9], the absolute change in sO_2 of blood samples in a container was quantified by fitting the temporal exponential rise in the detected PA signal. The advantage of this approach is self-calibration because the slope of the rise depends only on the relative change in the amplitude of the PA signal rather than the absolute values. However, this method relies on a large ultrasonic bandwidth because attenuation in blood is high, and requires that the surrounding tissue be geometrically simple and optically homogeneous. Thus, it has limited applicability to *in vivo* imaging. To measure sO_2 in small vessels *in vivo* with band-limited ultrasonic transducers, one has to develop a method to extract quantitative functional information from other features of PA signals.

In [12] and [13], *in vivo* two-dimensional mapping of sO_2 in both brain cortical vessels and subcutaneous vessels was reported. The smallest diameter of the imaged vessels is less than 50 μm . The advantage of this method is that band-limited ultrasonic transducers can be employed as long as the center ultrasonic wavelength is less than the optical penetration depth in blood [14]. In [12] and [13], two invasive methods were employed to measure the wavelength-dependent optical attenuation in the skin. The first method measured light transmission through a piece of exercised skin, whereas the second measured the PA spectrum of a subcutaneously inserted black (spectrally neutral) target *in vivo*. Because clinical applications prefer noninvasiveness, these invasive methods are impractical.

We found surprisingly that if the difference in sO_2 between neighboring vessels—rather than the absolute sO_2 in each vessel—is of interest, spectral compensation becomes inconsequential. Here, we first demonstrate numerically that the difference in sO_2 between subcutaneous vessels is minimally affected by the wavelength-dependent optical attenuation in the skin and then confirm our findings experimentally with *in vivo* PAM.

Experimental setup

The PAM system for the *in vivo* experiment was described in detail previously [6, 7]. This PAM system uses 6 ns pulses from a tunable dye laser. The ultrasonic detector has a center frequency of 50 MHz, a bandwidth of 80%, an active element diameter of 6.35 mm and a numerical aperture of 0.44. It is capable of imaging skin vasculatures at a depth of 3 mm with a lateral resolution of 45 μm , an axial resolution of 15 μm . The imaging system is sensitive enough to image blood vessels larger than 20 μm in diameter. Volumetric images are formed by a combination of recording of the time histories of PA signals and raster scanning of the ultrasonic detector. Vessels are isolated from the background according to their PA amplitudes and ultrasonic traveling times. Peak values of the PA signals that originated from vessels, after being normalized by the incident laser pulse energy, are used for a pixel-by-pixel calculation of the $s\text{O}_2$ in vessels only. Molar extinction coefficients of HbO_2 and HbR are taken from the literature [15, 16]. The effect of focal positioning of the ultrasonic transducer on the $s\text{O}_2$ measurement was found to be relatively small [14].

In *in vitro* studies, the PA peak amplitude has been demonstrated to have a linear dependence on the optical absorption coefficient (μ_a) when $\mu_a \Lambda < 1$, where Λ is the central wavelength of the ultrasonic transducer [14]. In phantoms made of cylindrical tubes filled with bovine blood, the $s\text{O}_2$ was quantitatively measured with high accuracy and sensitivity [13].

In this study, *in vivo* experiments were carried out in Sprague Dawley rats (~ 200 g, Charles River Breeding Laboratories, MA). The laboratory animal protocol for this work was approved by the Animal Studies Committee of Washington University in Saint Louis and all experimental animal procedures were carried out in conformity with the guidelines of the National Institutes of Health [17]. Changes of systemic physiological states in the experiment were achieved by varying the oxygen concentration of the inhalation anesthetic gas mixture as described in [13]. During the experiment, a pulse oximeter (8600 V, Nonin Medical, MN) was used to monitor the rat's arterial blood oxygenation and heart rate.

Model

The peak voltage A of a PA signal generated from a blood vessel at an optical wavelength λ is determined by the local optical fluence and several blood properties. Such properties (p_α) include oxygen saturation of hemoglobin $s\text{O}_2 = C_{\text{HbO}_2} / (C_{\text{HbR}} + C_{\text{HbO}_2})$ and total concentration of hemoglobin $C_{\text{Hb}} = C_{\text{HbR}} + C_{\text{HbO}_2}$, where C_{HbO_2} and C_{HbR} are the concentrations of HbO_2 and HbR in the blood, respectively. If A_k can be theoretically calculated from known p_α at λ_k , where k denotes the k th wavelength, the determination of $s\text{O}_2$ from the measured PA spectrum becomes a standard maximum likelihood parameter estimation problem. In fact, A also depends on other parameters such as the vessel geometry and the ultrasonic bandwidth. However, this dependence can be ignored within the spectral range of 550 nm and 650 nm [14].

Unfortunately, the local optical fluence can only be measured at the skin surface. Inside the skin, the fluence is depth dependent owing to optical scattering and absorption, where absorption is primarily due to melanin in the epidermis and hemoglobin in both the epidermis and dermis. The fluence distribution depends not only on the optical wavelength but also on the anatomical location and physiological state. To relate the optical fluence on the skin surface to the local fluence at a vessel, one may employ a complex skin model.

In this work, we use a simplified skin model [18, 19], which contains only two homogeneous layers: epidermis and dermis. Each layer is described by its thickness and

effective optical attenuation coefficient $\mu_{\text{eff}} = \sqrt{3\mu_a(\mu'_s + \mu_a)}$, where μ'_s denotes the reduced scattering coefficient. The optical fluence of an incident-collimated light beam is considered to attenuate exponentially through the skin. The wavelength dependence of the local fluence can be expressed as

$$F(\lambda) = F_0 \exp(-z_e \mu_{\text{eff}}^e(\lambda) - z_d \mu_{\text{eff}}^d(\lambda)), \quad (1)$$

where F_0 is the optical fluence on the skin surface; z_e and z_d are the layer thicknesses of the epidermis and dermis above the vessels to be imaged, respectively; and μ_{eff}^e and μ_{eff}^d are the effective optical attenuation coefficients in the epidermis and dermis, respectively. Although crude, this model gives a reasonable approximation of the optical fluence at depths larger than a few hundred micrometers [10].

The reduced optical scattering coefficients in both layers are assumed identical and expressed empirically as

$$\mu'_s = 1.1 \times 10^{12} \lambda^{-4} + 73.7 \lambda^{-0.22}, \quad (2)$$

where λ is in nm and μ'_s is in cm^{-1} [20]. The optical absorption coefficient in the epidermal layer μ_a^e is expressed empirically as

$$\mu_a^e = C_m 6.6 \times 10^{11} \lambda^{-3.33} + (1 - C_m) 7.84 \times 10^7 \lambda^{-3.255}, \quad (3)$$

where λ is in nm and μ_a^e is in cm^{-1} ; here, C_m denotes the volume fraction of melanosome, which varies from 1.3% to 43% depending on the skin color [15]. In our calculation, we use 5% for Sprague Dawley rats. Similarly, the optical absorption coefficient in the dermal layer is expressed as

$$\mu_a^d = C_B \mu_{aB}^d(\lambda) + (1 - C_B) 7.84 \times 10^7 \lambda^{-3.255}, \quad (4)$$

where C_B is the mean volume fraction of blood in the dermis; $\mu_{aB}^d(\lambda)$ is the optical absorption coefficient of blood in dermis. We have

$$\mu_{aB}^d = \{(\varepsilon_{\text{HbO}_2}(\lambda) - \varepsilon_{\text{HbR}}(\lambda)) \text{sO}_2^d + \varepsilon_{\text{HbR}}(\lambda)\} C_{\text{Hb}}, \quad (5)$$

where $\varepsilon_{\text{HbO}_2}$ and ε_{HbR} are the molar extinction coefficients of HbO_2 and HbR , respectively; sO_2^d is the spatially averaged oxygen saturation of hemoglobin in the dermis; and C_{Hb} is the hemoglobin concentration in the blood. In human skins, the typical value of C_B is about 0.2%. As a result, the optical absorption coefficient in the dermis is related to C_B , sO_2^d , $\varepsilon_{\text{HbO}_2}$ and ε_{HbR} .

The amplitude of the PA signal from a vessel located at depth $z_e + z_d$ can therefore be expressed as

$$A(\lambda) = K \mu_{aB} F(\lambda). \quad (6)$$

Here, K is a proportionality coefficient, which is related to the transducer sensitivity, ultrasound attenuation, detection geometry and Grüneisen coefficient [4]; and μ_{aB} is the local absorption coefficient of blood: $\mu_{aB} = \{(\varepsilon_{\text{HbO}_2}(\lambda) - \varepsilon_{\text{HbR}}(\lambda)) \text{sO}_2 + \varepsilon_{\text{HbR}}(\lambda)\} C_{\text{Hb}}$. From (6), it can be seen that only relative changes in C_{Hb} can be calculated quantitatively unless K is calibrated for.

The parameters discussed above are estimated by minimizing the difference between the experimental PA values $A_k^{(e)}$ measured at wavelength λ_k and the theoretical values $A_k(p_\alpha)$ in the least squares sense. Specifically, the following dimensionless relative error E^2 is minimized:

$$E^2 = \frac{\sum_k (A_k^{(e)} - A_k(p_\alpha))^2}{\sum_k (A_k^{(e)})^2}. \quad (7)$$

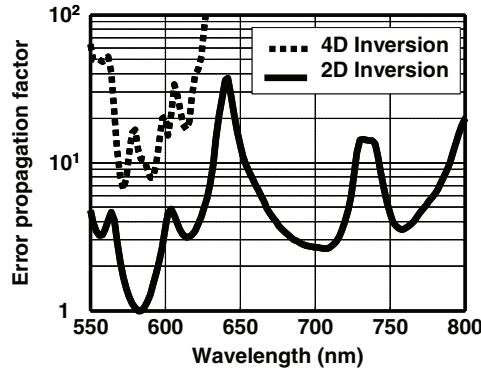


Figure 1. Error propagation factor for $s\text{O}_2$ inversion from PA signal amplitudes at expected values of $s\text{O}_2 = 1$, $s\text{O}_2^d = 0.8$ and $C_B = 0.004$. 4D, four-parameter inversion; 2D, two-parameter inversion.

We assume that all experimental measurements share a wavelength-independent normally distributed additive measurement error $\delta A_k^{(e)}$. The covariances of parameters p_α and $\delta p_\alpha/p_\alpha$ are related to the experimental errors by [14]

$$\sum_{\alpha,\beta} \frac{\delta p_\alpha}{p_\alpha} \left(\sum_k S_{\alpha k} S_{\beta k} \right) \frac{\delta p_\beta}{p_\beta} = \frac{\sum_k (\delta A_k^{(e)})^2}{\sum_k (A_k^{(e)})^2} = \frac{\eta}{n - \eta} \bar{E} F_{\eta, n-\eta}^{(1-\gamma)}. \quad (8)$$

Here,

$$S_{\alpha k} = \frac{\partial A_k}{\partial p_\alpha} \frac{p_\alpha}{(\sum_k A_k^2)^{1/2}}$$

is the sensitivity of the PA amplitude at the k th wavelength to parameter p_α ; \bar{E} is the residual value of E at convergence; $F_{\eta, n-\eta}^{(1-\gamma)}$, a constant of the order of unity, is an F -ratio distribution with $(\eta, n - \eta)$ degrees of freedom for a given confidence level, γ [21]; n is the number of wavelengths used; and η is the number of independent parameters.

Equation (8) defines an ellipsoidal surface in p_α space. Projection of the surface onto the p_A axis defines the normalized variance of parameter $\Delta p_A/p_A$. The ratio of $\Delta p_\alpha/p_\alpha$ to the residual error \bar{E} depends on the theoretical model that is used to calculate the PA signal and the expected parameters. This ratio gives an *a priori* estimate of the error propagation from the measurement of the parameter and is referred to as the error propagation factor (EPF) for p_α . The optimal choice of optical wavelengths used in experimental $s\text{O}_2$ measurements is defined by the condition of minimal error in $s\text{O}_2$ within limitations from the maximum tunable range of the dye laser. The number of wavelengths to be used should also be relatively small to keep the data-acquisition time reasonably short.

The EPFs as a function of optical wavelength for $s\text{O}_2$ in both a four-parameter inversion ($s\text{O}_2$, $s\text{O}_2^d$, C_B and $F_0 K C_{\text{Hb}}$ using eight wavelengths equally spaced by 3 nm) and a two-parameter inversion ($s\text{O}_2^d$ and C_B are fixed at 0.8 and 0.04, respectively, using only 4 wavelengths equally spaced by 6 nm) are shown in figure 1 against the shortest wavelength in the 18 nm window. The EPF minimum is about 7 for the four-parameter inversion but is about unity for the two-parameter inversion. In both cases, the minima occur in the wavelength range of about 570–590 nm, which is chosen for the *in vivo* experiment.

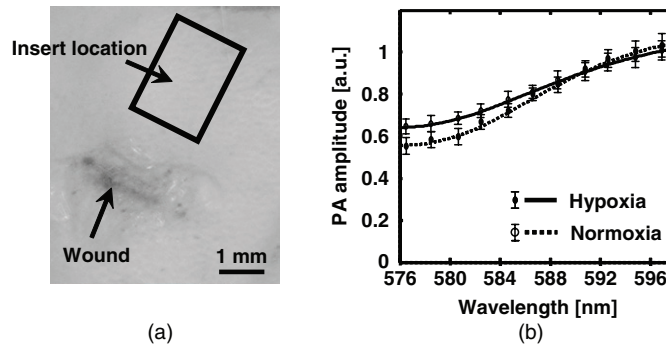


Figure 2. Experimental measurements of the optical fluence spectrum in rat skin by measuring the PA spectrum of a subcutaneously inserted black film *in vivo*. (a) Photo of insertion location of the black film. The rectangle indicates the approximate location of the black film. (b) Spectral dependence of the optical fluence attenuation in skin under hypoxia and normoxia.

Results and discussion

In our model, the values for $\varepsilon_{\text{HbO}_2}$, ε_{HbR} and C_m are taken from the literature; only C_B and $s\text{O}_2^d$ need to be estimated. To acquire meaningful values for C_B and $s\text{O}_2^d$, we fit equations (1) against the experimental data for the spectral dependence of the fluence decay in the rat skin. Experimental data were acquired using an invasive PA measurement. A $2 \text{ mm} \times 3 \text{ mm}$ rectangular piece of a $25 \mu\text{m}$ thick black polyethylene film was inserted under the rat skin beneath the dermis (figure 2(a)). The wound was sealed with surgical adhesive (NEXABAND, Closure Medical Corporation, NC). No bleeding or swelling was noticed around the insert. PA measurements were acquired under three physiological states: hyperoxia, normoxia and hypoxia. The black film insert was raster scanned by the PAM system with a step size of 0.05 mm at 12 wavelengths (from 576 nm to 598 nm with a 2 nm step). Before inserting the film, we measured the PA spectrum of the black film in an optically clear medium at the same optical wavelengths. No spectral variation in the PA amplitudes was observed, which indicated wavelength-independent optical absorption of the film within such a spectral range. Therefore, the acquired PA spectrum from the tissue represents the wavelength-dependent optical attenuation in the skin or the local wavelength-dependent fluence at the insert.

Figure 2(b) shows the fitted results for the black-film experiment. The experimental data are averaged from 96 points within an area of $0.3 \text{ mm} \times 0.8 \text{ mm}$. Lines in figure 2(b) correspond to the light attenuation according to equation (1) with the fitted C_B at 0.0033 and 0.0041 under hypoxia and normoxia, respectively. The $s\text{O}_2^d$ converged to 70% under hypoxia and exceeded 100% under normoxia. Therefore, $s\text{O}_2^d$ for normoxia was fixed at 100% level before inversion. For a group of two rats under the three physiological states, C_B varied between 0.21% and 0.53% , and $s\text{O}_2^d$ varied between 60% and $>100\%$. The total skin thickness $z_e + z_d$ was measured using the time of flight of the PA signal and the sound velocity in the skin. The thickness of the epidermis was assumed to be 0.1 mm . By fitting the PA spectrum from the black film insert with equation (6), we found that this simplified skin model described the optical effect of the skin on light propagation at the various optical wavelengths fairly well. In this case, both the residual error (an error in the model or a bias) and the standard deviation (a random error) are about 5% . Because the EPF for $s\text{O}_2$ in the four-parameter inversion is greater than 7, the expected error in the $s\text{O}_2$ inversion can exceed 35% , which means that simultaneous inversion for all vessel and tissue parameters is prone to large errors.

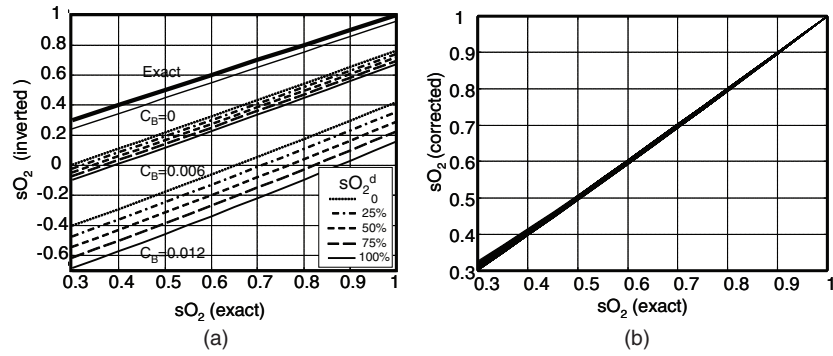


Figure 3. Influence of skin parameters on sO₂ estimation. (a) The three groups correspond to C_B values fixed at 0, 0.006 and 0.012. Within each group, separate curves are calculated for sO_2^d fixed at 0%, 25%, 50%, 75% and 100%. The thick diagonal line (top) represents the exact sO₂ values. (b) Results of sO₂ estimation after the linear empirical correction for the curves in panel (a). All groups of calculations fall into a range of variation of less than 1% for sO₂ values between 0.5 and 1.

Although the absolute sO₂ may not be measurable noninvasively *in vivo* with reasonable accuracy, it might be possible to quantify the relative changes in sO₂. First, we estimate the influence of sO_2^d and C_B ranging from 0 to 1 (all possible values) and 0 to 1.2% (more than twice the maximum measured value), respectively on the sO₂ inversion. For sO₂ ranging from 30% to 100%, we calculate $A_k(p_\alpha)$ at optical wavelengths 578, 584, 590 and 596 nm according to equation (6). We treat them as error-free experimental data and plot the result of the two-parameter ($F_0 K C_{Hb}$ and sO₂) inversion for sO₂ while completely ignoring light attenuation in the skin as shown in figure 3(a). As one can see, the skin optical attenuation defined by sO_2^d and C_B dramatically affects the inverted sO₂ value. However, the relationship of the inverted sO₂ values to the exact sO₂ values remains relatively linear. Moreover, the slopes of the curves in figure 3(a) do not change with sO_2^d and C_B as much as the absolute values of sO₂ do.

If *a priori* knowledge of sO₂ in some of the vessels is available, for example, if a blood vessel is known to be an artery from the morphology or the relatively high sO₂ (despite the initial inaccurate measurement) and its sO₂ is measured by some other technique such as pulse oximetry systemically, the changes in slope and bias among the curves in figure 3(a) can be minimized. For example, if the sO₂ in arterial blood under hyperoxia is 100%, a linear empirical formula can be constructed for such minimization. In this case, we found that the smallest deviation of the corrected sO₂ values from the exact data is obtained by using the following empirical formula:

$$sO_2 = 1 + (1 + 0.26sO_2^{(e)}(100\%))(sO_2^{(e)} - sO_2^{(e)}(100\%)). \quad (9)$$

Here, $sO_2^{(e)}(100\%)$ is the sO₂^(e) of arterial blood, and the empirical coefficient 0.26 depends on the chosen spectral range. The results after such a linear correction are shown in figure 3(b), where one can see that the bias of the two-parameter sO₂ inversion is decreased to less than ±1%.

Because $0 < sO_2^{(e)}(100\%) < 1$, coefficient $(1 + 0.26sO_2^{(e)}(100\%))$ in equation (9) varies by less than 20%, which means that the influences of sO_2^d and C_B on ΔsO_2 are more than 5-fold less than the influences on sO₂. Hence it can be assumed that, within reasonable bounds, at least relative changes in sO₂ (ΔsO_2) can potentially be quantitatively measured without prior knowledge of the skin optical properties. Such relative changes can be, for example,

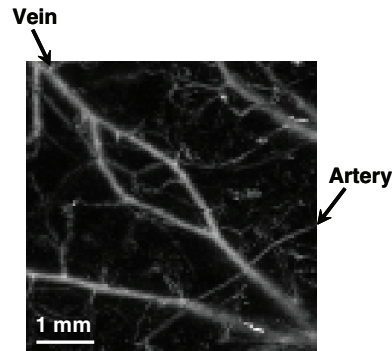


Figure 4. *In vivo* PAM image, where an artery and a vein are identified.

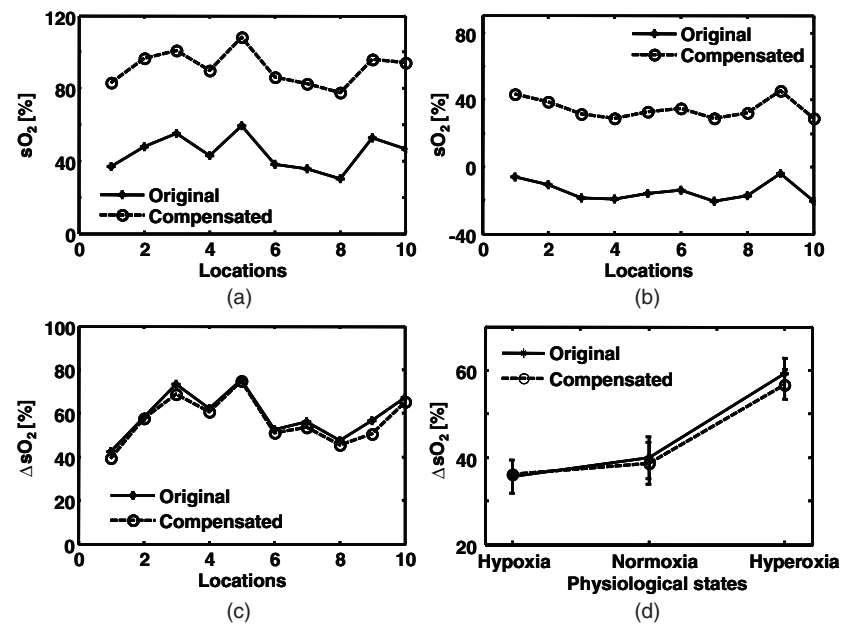


Figure 5. Comparison of sO_2 before and after spectral compensation in the selected artery (a) and vein (b) under hyperoxia. The ΔsO_2 under hyperoxia and the ΔsO_2 under three physiological states before and after spectral compensation are shown in (c) and (d), respectively.

between two neighboring vessels. Vessels are considered neighboring if they are separated by much less than the optical penetration depth (reciprocal of the optical effective attenuation coefficient).

To verify this assumption, we compared the sO_2 differences between a typical artery and a typical vein at multiple measurement locations before and after compensation for the spectral variation of the fluence at three physiological states *in vivo*. The calculation of sO_2 followed the description in [13, 14] and the PA spectrum of the black film was used as the spectral compensation factor at the corresponding optical wavelengths. As previously reported, arteries and veins can be separated using the imaged sO_2 ; we identified one artery and one vein as our target vessels in this work (figure 4). Ten measurement locations were then selected along each

vessel. At every location, sO_2 values before and after spectral compensation were calculated in both vessels.

As shown in figures 5(a) and (b), the two sets of sO_2 inversions are parallel to each other in both vein and artery, though the values obtained with spectral compensation are much more realistic. The ΔsO_2 between the vein and artery at the 10 measurements shows little dependence on the spectral compensation as well (figure 5(c)). The change of ΔsO_2 before and after spectral compensation is $2.42\% \pm 0.58\%$. Hence, it can be expected that even without spectral compensation, a reliable estimation of the variation in sO_2 can be experimentally achieved. Furthermore, ΔsO_2 was shown not to depend greatly on spectral compensation under all three physiological states (figure 5(d)). This observation demonstrates that functional parameters such as the local ΔsO_2 can be quantified noninvasively using PA measurement alone. Such a capability has potential applications in, for example, drug discovery for tumor treatment and brain functional study.

Conclusion

We have employed a simplified skin model, which contains only the epidermal and dermal layers. By approximating the fluence attenuation to an exponential decay with depth in each layer, we further model the PA amplitude generated from a vessel directly beneath the skin. By analyzing the error propagation with perturbations in various parameters in this model, we found that the absolute estimation of sO_2 based on PA measurement only is not feasible owing to the wavelength-dependent fluence attenuation in the skin. However, the difference in sO_2 between different vessels shows little dependence on such fluence attenuation. This conclusion is further supported by *in vivo* experimental results.

Acknowledgment

This research is sponsored in part by National Institutes of Health grants R01 CA106728 and R01 NS46214 (BRP).

References

- [1] Hoelen C G A, de Mul F F M, Pongers R and Dekker A 1998 Three-dimensional photoacoustic imaging of blood vessels in tissue *Opt. Lett.* **23** 648–50
- [2] Oraevsky A A and Karabutov A A 2003 *Optoacoustic Tomography in Biomedical Photonics Handbook* vol PM125 ed T Vo-Dinh (Boca Raton, FL: CRC Press)
- [3] Kruger R A, Liu P, Fang Y R and Appledorn C R 1995 Photoacoustic ultrasound (PAUS)—reconstruction tomography *Med. Phys.* **22** 1605–9
- [4] Xu M and Wang L V 2006 Photoacoustic imaging in biomedicine *Rev. Sci. Instrum.* **77** 041101
- [5] Wang X, Pang Y, Ku G, Xie X, Stoica G and Wang L V 2003 Noninvasive laser-induced photoacoustic tomography for structural and functional imaging of the brain *in vivo* *Nat. Biotechnol.* **21** 803–6
- [6] Maslov K, Stoica G and Wang L V 2005 *In vivo* dark-field reflection-mode photoacoustic microscopy *Opt. Lett.* **30** 625–7
- [7] Zhang H F, Maslov K, Stoica G and Wang L V 2006 Functional photoacoustic microscopy for high-resolution and noninvasive *in vivo* imaging *Nat. Biotechnol.* **24** 848–51
- [8] Zhang H F, Maslov K, Li M-L, Stoica G and Wang L V 2006 *In vivo* volumetric imaging of subcutaneous microvasculature by photoacoustic microscopy *Opt. Exp.* **14** 9317–23
- [9] Esenaliev R O, Larina I V, Larin K V, Deyo D J, Motamedi M and Prough D S 2002 Optoacoustic technique for noninvasive monitoring of blood oxygenation: a feasibility study *Appl. Opt.* **41** 4722–31
- [10] Laufer J, Elwell C, Depley D and Beard P 2004 *In vitro* measurements of absolute blood oxygen saturation using pulsed near-infrared photoacoustic spectroscopy: accuracy and resolution *Phys. Med. Biol.* **50** 4409–28

- [11] Laufer J, Deply D, Elwell C and Beard P 2007 Quantitative spatially resolved measurement of tissue chromophore concentrations using photoacoustic spectroscopy: application to the measurement of blood oxygenation and haemoglobin concentration *Phys. Med. Biol.* **52** 141–68
- [12] Wang X, Xie X, Ku G, Stoica G and Wang L V 2006 Non-invasive imaging of hemoglobin concentration and oxygenation in the rat brain using high-resolution photoacoustic tomography *J. Biomed. Opt.* **11** 024015
- [13] Zhang H F, Maslov K, Sivaramakrishnan M, Stoica G and Wang L V 2007 Imaging of hemoglobin oxygen saturation variations in single vessels in vivo using photoacoustic microscopy *Appl. Phys. Lett.* **90** 053901
- [14] Sivaramakrishnan M, Maslov K, Zhang H F, Stoica G and Wang L V 2007 Limitations of quantitative photoacoustic measurements of blood oxygenation in small vessels *Phys. Med. Biol.* **52** 1349–61
- [15] Jacques S L and Prahl S A 2004 Absorption Spectra for Biological Tissues (Oregon: Oregon Medical Laser Center) available online at <http://omlc.ogi.edu/spectra/hemoglobin/index.html>
- [16] Zijlstra W G, Buursma A and van Assendelft O W 2000 *Visible and Near Infrared Absorption Spectra of Human and Animal Hemoglobin, Determination and Application* (The Netherlands: VSP)
- [17] National Institute of Health Publication No. 86-23 1985 (Washington, DC: U.S. GPO)
- [18] Van Gemert M J C, Jacques S L, Sterenborg H J C M and Star W M 1989 Skin optics *IEEE Trans. Biomed. Eng.* **36** 1146–54
- [19] Jacques S L 1989 Skin Optics (Oregon: Oregon Medical Laser Center) available online at <http://omlc.ogi.edu/news/jan98/skinoptics.html>
- [20] Bashkatov I A N, Genina E A, Kochubey V I and Tuchin V V 2005 Optical properties of human skin, subcutaneous and mucous tissues in the wavelength range from 400 to 2000 nm *J. Phys. D: Appl. Phys.* **38** 2543–55
- [21] Lewicki P and Hill T 2006 Statistics Methods and Applications (Tulsa, OK: StatSoft Inc.)